Timing is Everything: Accurate, Minimum Overhead, Available Bandwidth Estimation in High-speed Wired Networks

Han Wang[1]
hwang@cs.cornell.edu

Ki Suh Lee[1]
kslee@cs.cornell.edu

Erluo Li[1]
erluoli@cs.cornell.edu

Chiun Lin Lim[2]
cl377@cornell.edu

Ao Tang[2]
atang@ece.cornell.edu

Hakim Weatherspoon[1]
hweather@cs.cornell.edu

[1]Department of Computer Science
Cornell University
Ithaca, NY 14850

[2]Department of Electrical and Computer Engineering
Cornell University
Ithaca, NY 14850

ABSTRACT

Active end-to-end available bandwidth estimation is intrusive, expensive, inaccurate, and does not work well with bursty cross traffic or on high capacity links. Yet, it is important for designing high performant networked systems, improving network protocols, building distributed systems, and improving application performance. In this paper, we present minProbe which addresses unsolved issues that have plagued available bandwidth estimation. As a middlebox, minProbe measures and estimates available bandwidth with high-fidelity, minimal-cost, and in userspace; thus, enabling cheaper (virtually no overhead) and more accurate available bandwidth estimation. MinProbe performs accurately on high capacity networks up to 10 Gbps and with bursty cross traffic. We evaluated the performance and accuracy of minProbe over a wide-area network, the National Lambda Rail (NLR), and within our own network testbed. Results indicate that minProbe can estimate available bandwidth with error typically no more than 0.4 Gbps in a 10 Gbps network.

1. INTRODUCTION

Active end-to-end available bandwidth estimation is intrusive, expensive, inaccurate, and does not work well with bursty cross traffic or on high capacity links [13, 33]. Yet, it is important [17, 43, 45]. It is necessary for designing high performant networked systems, improving network protocols, building distributed systems, and improving application performance.

The problems associated with available bandwidth estimation stem from a simple concept: Send a train of probe packets through a network path to momentarily congest the bottleneck link, then infer the available bandwidth at the

receiving end from probe packet timestamps [20, 36, 40, 46]. There are three significant problems with current bandwidth estimation approaches. First, such approaches are intrusive since load is being added to the network. Current measurement methods require creating explicit probe packets that consume bandwidth and CPU cycles. Second, current approaches often do not have enough fidelity to accurately generate or timestamp probe packets. By operating in userspace to maximize programming flexibility, precise control and measurement of packet timings is sacrificed. As a result, the probe packet timings are often perturbed by operating systems (OS) level activities. Without precise timestamps, accurate estimation becomes very challenging, especially in high-speed networks. Finally, Internet traffic is known to be bursty at a range of time scales [22], but previous studies have shown that existing estimation approaches perform poorly under bursty traffic conditions [48].

In this paper, we present a middlebox approach that addresses the issues described above. MinProbe performs available bandwidth estimation in real-time with minimal-cost, high-fidelity for high-speed networks (10 Gigabit Ethernet), while maintaining the flexibility of userspace control and compatibility with existing bandwidth estimation algorithms. MinProbe minimizes explicit probing costs by using application packets as probe packets whenever possible, while generating explicit packets only when necessary. MinProbe greatly increases measurement fidelity via software access to the wire and maintains wire-time timestamping of packets before they enter the host. Finally, a userspace process controls the entire available bandwidth estimation process giving flexibility to implement new algorithms as well as reuse existing estimation algorithms. Importantly, minProbe operates in real-time, such that it is useful as a networked systems building block.

MinProbe was designed with commodity components and achieves results that advance the state of the art. It can be built from a commodity server and an FPGA (field programmable gate array) PCIe (peripheral component interconnect express) pluggable board, SoNIC [26]. As a result, any server can be turned into a minProbe middlebox. Indeed, we have turned several nodes and sites in the GENI (global environment for networking innovations) network into minProbe middleboxes. It has been evaluated on a

	Low Fidelity Timestamping	High-Fidelity Timestamping
Active Probe	Pathload [20], Pathchirp [40], Spruce [46], TOPP [36]	minProbe
Passive Monitor	tcpdump	DAG [1]

Table 1: Bandwidth Estimation Design Space

testbed that consists of multiple 10 Gigabit Ethernet (10 GbE) switches and on the wide-area Internet via the National Lambda Rail (NLR). It achieves high accuracy: Results illustrate available bandwidth estimation with errors typically no more than 0.4 Gbps in a 10 Gbps network. It estimates available bandwidth with minimal overhead: Available bandwidth estimates use existing network traffic as probes. Overall, minProbe allows software programs and end-hosts to accurately measure the available bandwidth of high speed, 10 gigabit per second (Gbps), network paths even with bursty cross traffic, which is a unique contribution.

Our contributions are as follows:

• **High performance:** We are the first to demonstrate a system that can accurately estimate available bandwidth in 10 Gbps network.

• **Minimal overhead:** Albeit not the first middlebox approach to available bandwidth estimation(e.g. MGRP [37]), our system performs accurate bandwidth estimation with minimal overhead.

• **Ease of use:** Our system provides flexible userspace programming interface and is compatible with existing algorithms.

• **Sensitivity study:** We conduct a sensitivity study on our estimation algorithm with respect to internal parameter selection and network condition.

2. BACKGROUND

Available bandwidth estimation is motivated by a simple problem: What is the maximum data rate that a user could send down a network path without going over capacity? This data rate is equal to the available bandwidth on the *tight link,* which has the minimum available bandwidth among all links on the network path. While the problem sounds simple, there are four main challenges to available bandwidth estimation—timeliness, accuracy, non-intrusiveness, and consistency. In particular, an available bandwidth estimation methodology and tool would ideally add as little overhead as possible and return timely and accurate estimation on the available bandwidth consistently across a wide range of Internet traffic conditions.

In this section, we first discuss many of the key ideas and assumptions underlying existing available bandwidth estimation methods and tools. Then, motivate the development of minProbe by illustrating the limitations faced by these current methods and tools.

2.1 Methodology

Many existing available bandwidth estimation tools take an end-to-end approach. A typical setup sends probe packets with a predefined interval along the path under measurement, and observe change in certain packet characteristics
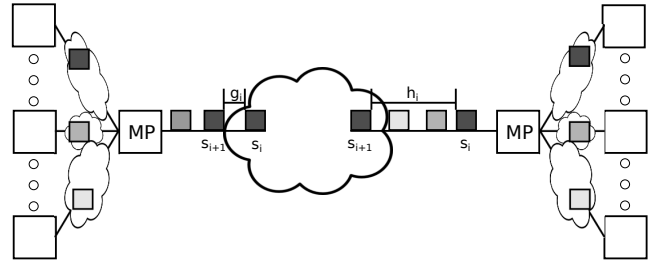

Figure 1: Usage of bandwidth estimation

at the receiver to infer the amount of cross traffic in the network. The key idea to such inferences: When the probing rate exceeds the available bandwidth, the observed packet characteristics undergo a significant change. The turning point where the change occurs is then the estimated available bandwidth. See Figure 9, for example, the turning point where queuing delay variance increases is the available bandwidth estimate. Most existing available bandwidth estimation tools can be classified according to the packet characteristics and metrics used to observing a turning point.

Bandwidth estimation tools such as Spruce [46] and IGI [16] operate by observing the change in the output probing rate. The idea is that when the probing rate is below the available bandwidth, probe packets should emerge at the receiver with the same probing rate. However, once the probing rate exceeds the available bandwidth, the gap between packets will be stretched due to queuing and congestion, resulting in a lower output probing rate. On the other hand, bandwidth estimation tools such as Pathload [20], PathChirp [40], TOPP [36], and Yaz [42] operate by observing the change in one-way delay (OWD), i.e. the time required to send a packet from source to destination. OWD increases when the probing rate exceeds the available bandwidth, as packets have to spend extra time in buffers.

An alternative methodology to the end-to-end approach would be to query every network element (switch/router) along a network path. A network administrator could collect the statistical counters from all related ports, via protocols such as sFlow [5]; or infer from Openflow control messages such as `PacketIn` and `FlowRemoved` messages [50]. However, obtaining an accurate, consistent, and timely reading from multiple switches in an end-to-end manner can be very difficult [2]. Further, collecting counters from switches is done at per-second granularity and requires network administrative privileges, which makes the approach less timely and useful for building distributed systems, improving network protocols, or improving application performance. As a result, we assume and compare to other end-to-end approaches for the rest of this paper.

2.2 Current Limitations

While useful, the end-to-end approach for available bandwidth estimation has inherent issues that limit its applicability, especially in high-capacity links. We outline a few of these challenges.

• **High-fidelity measurements require high-fidelity instruments.** Generating packet trains in userspace typically require a CPU-intensive busy-wait loop, which is prone to operating system level noise, such as OS scheduling, interrupt coalescing, and batching. As a result, generated interpacket gaps of a packet train rarely match the interpacket

gaps specified by the userspace program. Moreover, timestamping in user or kernel space adds considerable error to the available bandwidth estimation. Even timestamping in hardware adds noise when timestamping packet (albeit, less noise than kernel space, but still enough to make available bandwidth estimation unusable in many situations [27]). The takeaway: Without high-fidelity capabilities, available bandwidth estimation lacks accuracy.

• **Non-negligible overhead.** Bandwidth estimation tools add traffic to the network path under measurement. This may adversely affect application traffic and measurement accuracy [37]. The amount of probe traffic is proportional to the rate of sampling and the number of concurrent measurement sessions. As a result, the effect of probe packets on cross traffic exacerbates with traffic increase.

• **Traffic burstiness impacts measurement results.** Bandwidth estimation results are sensitive to traffic burstiness. However, existing tools typically ignore the burstiness of cross traffic in favor of simple estimation algorithms. Limitations of batching and instrumentation further mask burstiness to some degree to userspace tools. As a result, existing tools may not be able to reflect true available bandwidth with bursty traffic.

In this paper, we introduce a new tool that can be applied to existing available bandwidth estimation algorithms and tools while overcoming the limitations discussed above. Indeed, we demonstrate that we can accurately estimate available bandwidth in high-speed networks with minimal overhead with existing algorithms. In the next section, we discuss the details of the design and implementation of our methodology.

3. MinProbe DESIGN

MinProbe measures the available bandwidth with high-fidelity, minimal-cost and in userspace; thus, enabling cheaper (virtually no overhead) and more accurate available bandwidth estimation. It achieves these goals through three main features:

First, minProbe is a middlebox architecture that uses application network traffic as probe traffic to eliminate the need for explicit probe packets. When an application packet arrives at minProbe, minProbe decides whether the packet should be used as a probe; if so, minProbe modulates the timings between application packets chosen as probe packets before forwarding them to their destination. A programmable flow table accessible from userspace controls the selection of an application packet as a probe packet. Thus, by using application traffic implicitly as available bandwidth probes, we are able to remove all the traditional costs and overheads. A similar idea was proposed in MGRP [37], which has the same goal of lower overhead, but MGRP lacks high-fidelity measurement capability.

Second, minProbe is a high-fidelity network measurement substrate that is capable of modulating and capturing traffic timings with sub-nanosecond precision. The high-precision is achieved by enabling software access to the physical layer of the network protocol stack. When minProbe modulates probe packets (application packets), it adds and removes minute spacings between packets through direct access to the physical layer.

Finally, minProbe is accessible from userspace. From userspace, users can control sub-nanosecond modulations

between packets to generate probes and obtain sub-nanosecond timings between received packets to estimate available bandwidth. Further, all probes can be generated and timing measurements can be received in real-time from userspace.

We envision minProbe to be deployed in an architecture where a separate control plane manages a rich set of middlebox functionalities with event trigger support(e.g [9]). In particular, we believe the separation of measurement hardware and production hardware enables high-fidelity measurement in high-speed networks (and in real-time) that is difficult to achieve otherwise.

3.1 Precise Probe Control

MinProbe offers enhanced network measurement capabilities: High-fidelity packet pacing to generate probe packets and high-fidelity packet timestamping to measure received packet times. We achieve high-fidelity capabilities via direct access to the physical layer from software and in real-time. To see how minProbe works, we first describe the physical layer of 10 Gigabit Ethernet (GbE). Then, we describe how minProbe takes advantage of the software access to the physical layer to achieve high-fidelity network measurement.

3.1.1 10 GbE Physical Layer

According to the IEEE 802.3 standard [3], when Ethernet frames are passed to the physical layer (PHY), they are re-formatted before being sent across the physical medium. On the transmit path, the PHY encodes every 64bits of an Ethernet frame into a 66bit *block*, which consists of a two bit *synchronization header* (sync-header) and a 64bit *payload*. As a result, a 10 GbE link actually operates at 10.3125 Gbaud ($10G \times \frac{66}{64}$). The PHY also scrambles each block before passing it down the network stack to be transmitted. The entire 66bit block is transmitted as a continuous stream of *symbols*, which a 10 GbE network transmits over a physical medium. As 10 GbE always sends 10.3125 gigabits per second (Gbps), each bit in the PHY is about 97 pico-seconds wide. On the receive path, the PHY layer removes the two-bit header and de-scrambles each 64bit block before decoding it.

Idle symbols (/I/) are special characters that fill the gaps between any two packets in the PHY. When there is no Ethernet frame to transmit, the PHY continuously inserts /I/ symbols until the next frame is available. The standard requires at least twelve /I/s after every packet. Depending on Ethernet frame and PHY alignment, an /I/ character can be 7 or 8 bits, thus it takes about 700∼800 pico-seconds to transmit one /I/ character [3]. Importantly, controlling or simply counting the number of /I/s between packets is what enables high-fidelity. However, before the SoNIC [26] platform was created, /I/ characters were typically inaccessible from higher layers (L2 or above), because they are discarded by hardware, and definitely were not accessible in software.

3.1.2 High-Fidelity Measurement

The key insight and capability of how minProbe achieves high-fidelity is from its direct access to the /I/ characters in the physical layer. In particular, minProbe can measure (count) and generate (insert or remove) an exact number of /I/ characters between each subsequent probe packet to measure the relative time elapsed between packets or generate a desired interpacket gap. Further, if two subsequent probe packets are separated by packets from a different flow
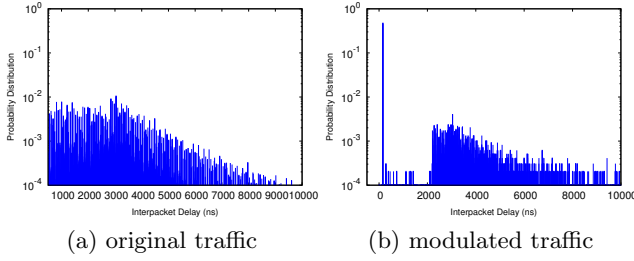
(a) original traffic　　(b) modulated traffic

Figure 2: Comparison of traffic pattern before and after passed through middlebox

(*cross traffic*), the gap between probe packets will include `/I/` characters as well as data characters of the cross traffic packets, but the measurement will still be exact (i.e. `/I/` and data characters represent time with sub-nanosecond precision). This level of access from software is unprecedented. Traditionally, however, an end host may timestamp packets in userspace, kernel, or network interface hardware which all add significant noise. None of these methods provide enough precision for high-fidelity network measurements; consequently, many existing bandwidth estimation tools report significant estimation error (large variation and low accuracy) [27].

In a similar fashion to measuring the space between packets, minProbe generates probe packets through high-fidelity pacing, by inserting an exact spacing between packets. By accessing the physical layer of 10 GbE in software in real-time, minProbe can insert or remove `/I/` characters from application traffic as needed. In particular, two variables of the probe traffic are of interest: The gap between packets and the overall rate of packet trains. Users can program minProbe via command line calls or API calls to specify the number of `/I/` characters (i.e. the number of 100s of pico-seconds) to be maintained between subsequent probe packets, allowing userspace programs to perform high-fidelity pacing.

Direct access to `/I/` characters from software and in real-time differentiates minProbe from other measurement tools. Specifically, minProbe is able to characterize and generate an *exact* spacing (interpacket gap) between probe packets.

3.1.3　Probing without a Probe

Explicit probes are not necessary for minProbe. Similar to MGRP [37], minProbe can use application traffic as probe packets. It has a programmable flow table that performs flow matching on pass-through traffic. Users can insert entries into the flow table to specify which flows are probes. Traffic that have a match in the flow table are modulated before they are forwarded. Other flows that do not have a match are simply forwarded without any change in timing. With minProbe, we are able to perform line-rate forwarding at 10 Gbps, even for the minimum size packets. Moreover, minProbe has the ability to generate explicit probe packets, especially when there is insufficient application traffic. Dummy probing packets are padded with zero bytes and transmitted at pre-defined intervals as programmed by the users.

Figure 2 illustrates minProbe's ability to perform high-fidelity measurement and pacing as a middlebox with only application packets as probes. Figure 2a shows the distribution of incoming application traffic to a minProbe mid-

dlebox. The x-axis is the distance in time between the first byte of subsequent packets (or *interpacket delay*), and y-axis is the frequency of occurrences. We generated two flows of application traffic at 1 Gbps, and a minProbe middlebox was configured to only modulate one of the flows. As can be seen in Figure 2b, after minProbe, the packets of the probing flow have minimal spacing (interpacket delay) between subsequent packets, and exhibit a much higher probe rate: The peak just to the right of 0 ns interpacket delay was the modulated probing traffic. Even though the overall application traffic rate was 1 Gbps, we were able to increase the instantaneous probe rate up to 10 Gbps for short periods of time by creating short packet trains with minimal interpacket delay. The packets of the other flows, on the other hand, were forwarded as-is, with no changes in timing.

How would minProbe impact the application traffic performance? Obviously, if any traffic were paced, then minProbe would change the pacing. But, for general TCP traffic, the minute modulation that minProbe causes does not affect the rate or TCP throughput. Similar results have been demonstrated in prior art MGRP [37]. One problem may occur when a TCP cwnd (congestion window) is small, e.g., when cwnd = 1. In this case, the application does not create enough traffic and dummy probe needs to be created.
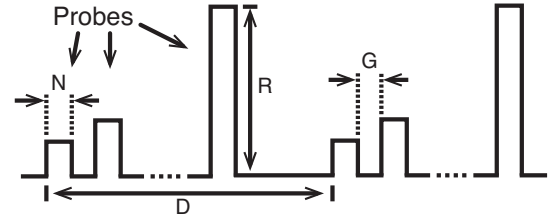
3.2　Generalized Probe Model

Figure 3: Generalized probe train model

Figure 3 shows a generalized probe train model we developed to emulate a number of existing bandwidth estimation algorithms and used for the rest of the paper. The horizontal dimension is time. The vertical dimension is the corresponding (instantaneous) probe rate. Each pulse (we call it a *train*) contains multiple probe packets sent at a particular rate, as depicted by the height. In particular, the parameter N represents the number of packets in each train and parameter R represents the (instantaneous) probe rate of the train (i.e. we are able to change the interpacket gap between N packets to match a target probe rate R). Packet sizes are considered in computing the probe rate. For a mixed-size packet train, minProbe is able to adjust the space between all adjacent packets within the train to achieve the desired probe rate R. The gaps between successive probe trains are specified with parameter G (gap). Finally, each measurement *sample* consists of a set of probe trains with increasing probe rate. The distance in time between each measurement sample is identified with parameter D (distance). With these four parameters, we can emulate most probe traffic used in prior work, as shown in Table 2 and discussed in Section 2.1. For example, to emulate Spruce probes, we can set the parameters (N, R, G, D) to the values (2, 500Mbps, 1.2ns, 48us), which would generate a pair of probe packets every 48 us with minimal inter-packet gap (12 `/I/` characters or 1.2ns) at 500Mbps (5% of the capacity of a 10Gbps link), as in-

Algorithm	N	R	G	D
Pathload	20	[0.1:0.1:9.6] Gbps	Variable	Variable
Pathchirp	1	[0.1:0.1:9.6] Gbps	Exponential decrease	Variable
Spruce	2	500Mbps	1.2ns	48us
IGI	60	[0.1:0.1:9.6] Gbps	30s	30s

Table 2: Parameter setting for existing algorithms. G is the gap between packet trains. R is the rate of probe. N is the number of probe packets in each sub-train. D is the gap between each sub-train.

tended by the original Spruce Algorithm [46]. Similarly, to reproduce the IGI experiment results [16], we set the parameters (N, R, G, D) to the values (60, [0.1:0.1:9.6]Gbps, 30s, 30s) to generate probe trains of 60 packets every 30 seconds with rate ranging from 100Mbps to 9.6Gbps at 100Mbps increments. In summary, most types of existing probe trains can be emulated with the generalized model we developed for minProbe, where different points in the parameterization space can represent different points in the entire design space covering prior art and possibly new algorithms.

In the following sections, we use a parameterization that is similar to Pathload, which estimates available bandwidth based on the increasing one-way delay (OWD) in probe trains. If the rate of a probe train is larger than the available bandwidth of the bottleneck link, the probe train will induce congestion in the network. As a result, the last packet of the probe train will experience longer queuing delays compared to the first packet of the same probe train. The difference between the OWD of the last packet and the first packet of the same probe train can be used to compute the increasing OWD in the probe train. On the other hand, if a probe train does not induce congestion, then there will be no change in the OWD between the first and last packet. Thus, if an available bandwidth estimation algorithm sends probe trains at different rates R, it will estimate the available bandwidth to be the lowest probe train rate R where the OWD (queuing delay) increases.

A bandwidth estimation algorithm based on Pathload needs to measure the change (increase) in OWD between the first and last packet in a probe train. Since we can measure the gaps between subsequent packets, we show that the interpacket gap information is sufficient to compute the increase in the OWD of a probe packet train.

PROOF. Consider sending a train of n packets with packet sizes $s_1, s_2, \ldots, s_n$ and interpacket gaps $g_1, g_2, \ldots, g_{n-1}$ from host A to host B through a network path. The received packets at host B experiences one-way delays of $q_1, q_2, \ldots, q_n$ through the network and now have interpacket gaps $h_1, h_2, \ldots, h_{n-1}$. Assume no packet losses due to network congestion, and no packet reordering in the network. Then we want to show that the difference in one-way delay of the first and last packets is equal to the total increase in interpacket gaps, i.e. $q_n - q_1 = \sum h_i - \sum g_i$.

Initially, the length of the packet train measured from the first bit of the first packet to the last bit of the nth packet is given

$$l^A = \sum_{i=1}^{n-1} g_i + \sum_{j=1}^{n} s_j \qquad (1)$$

Similarly at the receiving end

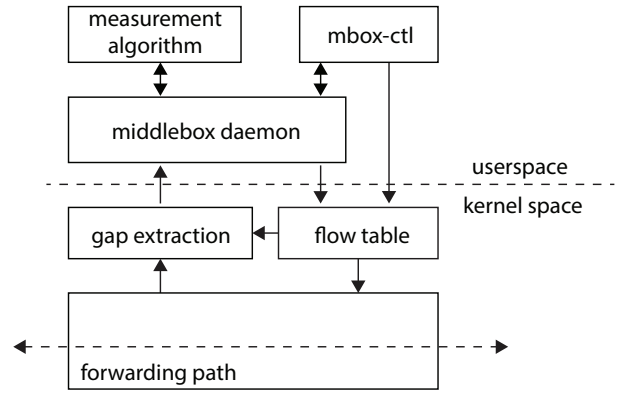$$l^B = \sum_{i=1}^{n-1} h_i + \sum_{j=1}^{n} s_j \qquad (2)$$

Figure 4: MinProbe Architecture

Additionally, the difference in one-way delay tells us that

$$l^B = l^A + (q_n - q_1) \qquad (3)$$

Substitute the relationship for l^A and l^B and we can see that the difference in one-way delay is equivalent to the difference of interpacket gap. $\square$

3.3 Implementation

We built a prototype of minProbe on the software network interface, SoNIC, platform with two 10 GbE ports [26]. The detailed design of the SoNIC platform has been described in prior work [26]. Here, we briefly recount the main features of SoNIC. SoNIC consists of two components: a software stack that runs on commodity multi-core processors, and a hardware PCIe pluggable board. The software implements all of the functionality in the 10GbE physical layer that manipulates bits to enable access to `/I/` in software. The hardware performs line-speed data transfer between the 10 GbE transceiver and the host. To enable the high-fidelity network measurements required by minProbe, we extended SoNIC's capabilities with three new features:

Packet Filtering and Forwarding: We extended SoNIC to support packet forwarding and filtering at line rate. Packet forwarding preserves the timing characteristics of the pass-through traffic exactly: Data is copied from an incoming port to an outgoing port, including the exact number of `/I/` characters in between each packet. To filter for probe packets, we use an in-kernel flow table that matches on the 5-tuples of a packet IP header. The packets that have a match are temporarily buffered in a queue, interpacket gap modulated, and sent once enough packets have been buffered for a single packet train (a measurement sample).

Packet Gap Extraction and Manipulation: MinProbe has two operational modes: a modulation mode for sending probes and an extraction mode for receiving probes. In the modulation mode, we extended SoNIC with additional packet queues for temporarily buffering of probe packets, and modified the amount of `/I/` characters in front of the buffered packet to change the packet spacing. If `/I/` characters are removed from the probe packet trains to increase the probe rate, we compensate for the loss of `/I/` characters at the end of the probe packet train to conform to the 10 GbE standard, and vice versa. In the extraction mode, the number of `/I/` characters are extracted from the matched probe packet trains and sent to the userspace programs via kernel upcalls.

Function	Description	Example
set_mode	set middlebox mode	set_mode
set_gap	set gap between probes	set_gap(120,120,120)
flow_add	add flow used as probes	flow_add(srcip,dstip)

Table 3: Application Programming Interface

Application Programming Interface: The last feature we added was the userspace accessibility. Users can insert/remove flow entries, dynamically adjust probe packet gaps, and retrieve probe packet gap counts from minProbe. It is required to implement a flexible user and kernel space communication channel for passing measurement data and control messages between user and kernel space. We used the *netlink* [4] protocol as the underlying mechanism and implemented the exchange of information using netlink messages. For example, we encapsulate the interpacket gaps in a special netlink message, and transmitted it from kernel to userspace, and vice versa.

Userspace daemons control minProbe. Userspace daemons provide a programmable interface for the kernel-to-user datapath. Table 3 presents a few API calls that are supported by minProbe. For example, as shown in Figure 4, users can program the flow table through the daemon or directly by `flow-add` commands. In addition, users can retrieve information from the kernel through the userspace daemon. In particular, a kernel module captures the interpacket gap /I/ counts from the probe traffic and passes the information to userspace through the userspace daemon. All communication consumes a reasonably small amount of bandwidth. For instance, the most expensive action is the transfer of interpacket gap /I/ counts from kernel to userspace, which requires a few hundred mega-bytes per second of bandwidth for minimum sized 64 byte packets at 10 Gbps.

4. EVALUATION

MinProbe can accurately estimate the available bandwidth in high-speed networks with minimal overhead. To demonstrate its capabilities and accuracy, we evaluated minProbe over three different physical networks: Two topologies in our controlled environment and the National Lambda Rail (NLR). We used a controlled environment to study the sensitivity of estimation accuracy to various network conditions. We also evaluated minProbe on NLR to study its performance in wide area networks. To highlight the accuracy minProbe is capable of, Figure 8 in Section 4.2 shows that minProbe can accurately estimate the available bandwidth within 1% of the actual available bandwidth in a 10Gbps network with topology shown in Figure 6a.

In the remainder of this section, we evaluate minProbe in depth and seek to answer the following questions:
- How *sensitive* is minProbe to application and cross traffic characteristics (Section 4.3 and 4.4)?
- Does minProbe work in the wild (Section 4.5)?
- Can other software middleboxes accurately measure available bandwidth (Section 4.6)?

4.1 Experimental setup

Our evaluation consists of two parts: Controlled environment experiments and wide area network (WAN) experiments. For the WAN experiments, we evaluate minProbe over the National Lambda Rail (NLR). NLR is a transcontinental production 10Gbps Ethernet network shared by research universities and laboratories with no restriction on
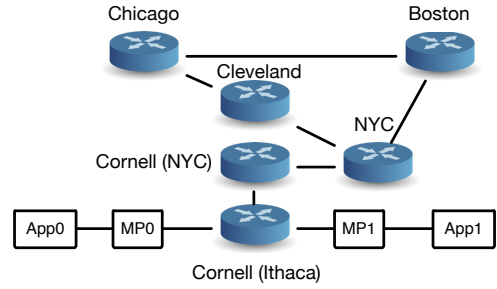

Figure 5: National Lambda Rail Experiment
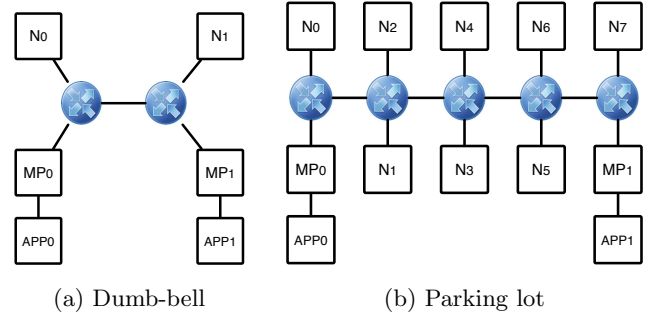

(a) Dumb-bell   (b) Parking lot

Figure 6: Controlled Experiment Topologies

usage or bandwidth. As a result, traffic in the NLR is typically bursty, yet persistent, and similar to the Internet. We provisioned a dedicated virtual route that spans nine routing hops over 2500 miles, as shown in Figure 5. Since the underlying physical network is also shared with other provisioned routes, we observed persistent cross traffic between 1 Gbps to 3.5 Gbps.

For the controlled environment experiments, we set up two different network topologies in a 10 Gbps network testbed: Dumb-bell (DB) and parking-lot (PL), as illustrated in Figure 6 and described in [49]. We used one minProbe middlebox (MP_0) to modulate the application traffic generated from a server directly connected to MP_0. We used the other minProbe middlebox (MP_1) as the receiver of the modulated probes to capture the timing information from the application traffic. A network of one or more hops separated the two middleboxes, where one link was a bottleneck link (i.e. a tight link with the least available bandwidth). Our experiments attempted to measure and estimate the available bandwidth of this bottleneck (tight) link. The testbeds were built with commercial 10 GbE switches, represented by circles in Figure 6. MinProbe middleboxes and hosts that generated cross traffic were separately connected to the switches using 10 GbE links, illustrated with the solid line. In the DB topology, the link between the two switches is the bottleneck (tight) link. In the PL topology, the bottleneck (tight) link depends on the pattern of the cross traffic.

MP_0 and MP_1 were Dell PowerEdge T710 servers. Each server had two Intel Xeon Westmere [19] X5670 2.93GHz processors, with six cores in each CPU and a total of 24 GB RAM. The Westmere architecture of the processor is well-known for its capability of processing packets in a multi-threaded environment [11, 14, 35]. The switches used in the environment consisted of an IBM G8264 RackSwitch and

(a) CAIDA OC-192 trace

(b) Energy plot for CAIDA trace

(c) Synthesized traffic

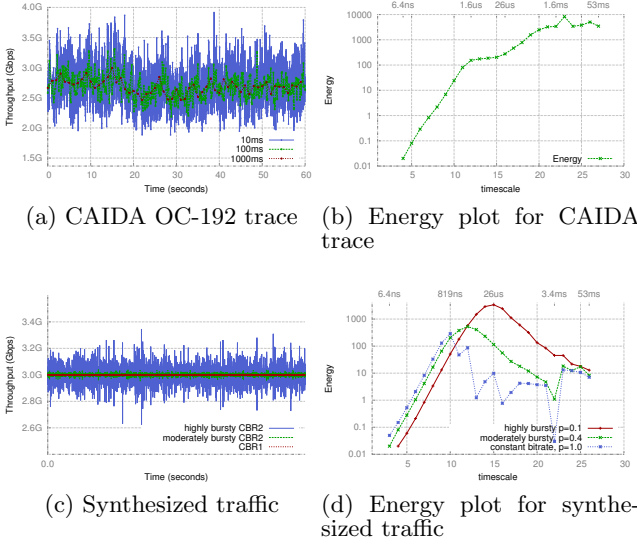(d) Energy plot for synthesized traffic

Figure 7: The time series and wavelet energy plots for cross traffic used in controlled experiments. Figure 7a shows a time series of a CAIDA trace in three different time scales: 10ms, 100ms and 1s. Coarser time scale means longer averaging period, hence less burstiness. Figure 7b shows the corresponding wavelet energy plot for the trace in Figure 7a. Figure 7c shows three different traces with different traffic burstiness of the same time scale. Figure 7d shows the corresponding wavelet energy plot, with higher energy indicating more burstiness.

a Dell Force10 switch, with network divided into separate logical areas using VLANs.

We used three different classes of cross traffic for our controlled experiments. Figure 7 illustrates the time series characteristics of all three traffic classes. The different classes of cross traffic are also described below.

Constant bit rate cross traffic (CBR1): CBR1 cross traffic consists of fixed-sized and uniformly distributed packets. In particular, CBR1 traffic is a stationary traffic with constant average data rate over long time scale (milliseconds), and interpacket gaps are uniform (i.e., variance is zero).

Stationary, but bursty cross traffic (CBR2): The second class of cross traffic was generated from stationary but bursty distributions, CBR2. CBR2 is created by varying both the packet size and packet chain length distributions with two parameters $\mathcal{D}_{size}$ and $\mathcal{D}_{len}$. Both parameters range from 0.0 (zero variance) to 1.0 (high variance). We draw the packet size from a log-normal distribution which has been demonstrated to closely resemble the distribution of Internet traffic in [28]. The mean of the log-normal distribution is fixed, while the variance is controlled by the parameter $\mathcal{D}_{size}$ to be $\mathcal{D}_{size} \cdot \mathcal{V}_{size}$, where $\mathcal{V}_{size}$ is a fixed high variance value. A packet chain is a series of consecutive packets with minimal interpacket gap in between, and from [12], we know its length takes on a geometric distribution. The parameter of the geometric distribution is taken to be $1 - \mathcal{D}_{len}$. Thus, CBR1 is a special case of CBR2 where both $\mathcal{D}_{size}$ and $\mathcal{D}_{len}$ equals 0.0.

Packet size [Bytes]	Data Rate [Gbps]	Packet Rate [pps]	IPD [ns]	IPG [/I/]
792	1	156250	6400	7200
792	3	467814	2137	1872
792	6	935628	1068	536
792	8	1250000	800	200

Table 4: IPD and IPG of uniformly spaced packet streams.

CAIDA: In the third scheme, we generated cross traffic from a real internet trace. In particular, we used the CAIDA OC-192 [6] trace which was recorded using a DAG card with nano-second scale timestamps.

While there is not one commonly accepted definition for traffic burstiness in the literature, burstiness generally refers to the statistical variability of the traffic. In other words, high variability in traffic data rates implies very bursty traffic. Variability, and by extension, traffic burstiness could be captured by wavelet-based energy plot [47]. Specifically, the energy of the traffic represents the level of burstiness at a particular timescale (e.g. at the microsecond timescale). The higher the energy, the burstier is the traffic. Figure 7b and 7d illustrate this wavelet-based energy plot when applied to the byte arrivals for CAIDA Internet traces and synthetically generated traffic, respectively. The x-axis represents different time scale, ranging from nano-second to second in log scale. The y-axis represents the abstracted energy level at a particular time scale. We were mostly interested in the micro-second timescale, which correspond to x-axis values around 15. Notice that the synthetic traffic behave very much like CAIDA internet traces for energy levels for these values.

For most experiments, we used 792 bytes as the application traffic packet size, which according to [6], is close to the average packet size observed in the Internet. We adjusted the traffic data rate by varying interpacket gaps (IPG). In particular, we insert a specific number of /I/'s between packets to generate a specific data rate. We controlled the exact data rate of CBR1 and CBR2 since we control the exact number of /I/'s inserted between packets. However, for the CAIDA traces, we selected portions of the trace recording times to obtain different average data rates. In addition, when we replay a trace, we only need to preserve the timing information of the trace, not the actual payload. We used SoNIC to replay the CAIDA trace. As described in [26], SoNIC can regenerate the precise timing characteristics of a trace with no deviation from the original.

4.2 Baseline Estimation

How does available bandwidth estimation perform using minProbe in a base case: A simple topology with a couple to several routing hops (Figure 6.a and b) and uniform cross traffic (uniform packet size and interpacket gaps)? We illustrate the result with the following experiments.

In the first experimental network setup, we use a dumbbell topology with two routing hops and a single bottleneck link (Figure 6a). Cross traffic is generated with a constant bit rate that has uniform packet sizes and interpacket gaps (CBR1). Node N_0 sends cross traffic to node N_1 according to the CBR1 uniform distribution.

The second experimental setup is similar to the first except that we use a parking-lot topology (Figure 6b). Further, cross traffic is generated with the CBR1 uniform distribution between neighboring nodes: N_{even} to N_{odd} (e.g. N_0 to
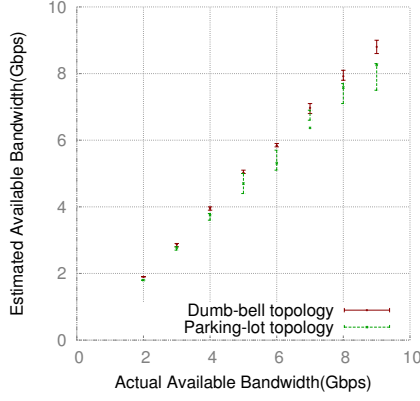
Figure 8: Available bandwidth estimation in a dumb-bell and parking-lot topology under CBR traffic. Both cross traffic and probe traffic share one bottleneck with the capacity of 10Gbps. The x-axis represents the actual available bandwidth of the bottleneck link. The y-axis represents the estimation by minProbe. This evaluation demonstrates min-Probe's ability to accurately measure the available bandwidth and achieve the estimation with minimal probing overhead.

N_1, N_2 to N_3, etc). Thus, we can control the cross traffic separately on each link.

In all experiments, we varied the data rate of the CBR1 cross traffic from 1 Gbps to 8 Gbps with an increment of 1 Gbps each time. We configured MP_0 to modulate application traffic from APP_0 destined to APP_1 to create probe packet samples. Note that there is no overhead since we are not introducing any new packets. Further, we configured MP_1 to capture the timing information of the probe packet samples (i.e. application traffic destined to APP_1 from source APP_0). The probe packets modulated by MP_0 were parameterized using the model introduced in Section 3.2. We used the parameters $(N, R, G, D) = (20, [0.1 : 0.1 : 9.6]$ Gbps, 10 us, 4 ms) where MP_0 sends a probe packet sample every 4 ms enabling us to collect 250 samples per second. Each probe sample consists of 96 constant bit rate (CBR) trains with a 10 us gap between trains. Each train runs at an increasing data rate ranging from 0.1 Gbps to 9.6 Gbps, with an increment of 0.1 Gbps. Recall that we are able to precisely control the data rate of trains by controlling the interpacket gap between probe packets within the train (e.g. See Table 4). We assume node APP_0 generates enough application traffic to create probe packet samples.

Figure 8 shows the result. It shows the actual available bandwidth on the x-axis and estimated available bandwidth on the y-axis for the the dumb-bell and parking-lot topologies. We estimated the available bandwidth with the mean of 10 measurement samples. The estimations in the dumb-bell topology were within 0.1 Gbps of the actual available bandwidth. The estimations in parking-lot topology tended to under-estimate the available bandwidth, due to the multiple bottleneck links in the network path. Higher available bandwidth scenarios were more difficult to measure as accurately in a multiple-hop network path. Alternatively, the maximum value of a measurement could be used to estimate available bandwidth if the estimation was always overly conservative; this would actually increase the estimation accuracy.

Figure 9 shows the raw probe sample data that was used to estimate the available bandwidth of different cross traffic
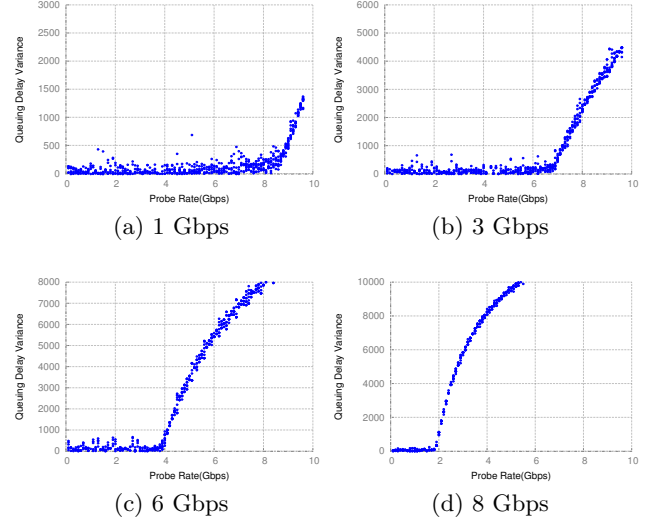

(a) 1 Gbps

(b) 3 Gbps

(c) 6 Gbps

(d) 8 Gbps

Figure 9: Scatter-plot showing the queuing delay variance of probe packets versus the probe rate. The cross traffic rate are constant at 1Gbps, 3Gbps, 6Gbps and 8Gbps. We used probe with N=20, R=[0.1:0.1:9.6]Gbps, G=10us, D=4ms.

rates in the dumb-bell topology. The x-axis is the rate (R) at which the probe trains were sent. The y-axis is the variance of the queuing delay, which was computed from the one-way delay (OWD) experienced by the packets within the same probe train. We kept the cross traffic rate constant at 1Gbps, 3Gbps, 6Gbps and 8Gbps. The available bandwidth was estimated to be the turning point where the delay variance shows an significant trend of increasing.

4.3 Impact of Application Traffic

Next, we study whether minProbe is impacted by characteristics of application traffic. In particular, we focus on two characteristics that matter the most for available bandwidth estimation: the length of a probe train and the distribution of probe packet sizes. The length of a probe train affects the delay experienced by application traffic (See the description of probe train length in Section 3.2 and equation 1). The longer the probe train, the longer the application traffic has to be buffered in the middlebox, resulting in longer delays the application traffic experiences. Typically, a probe train consists of around 100 or more packets [20, 40]. A probe train of two packets is essentially similar to the packet pair scheme described by Spruce [46].

Creating probe packet trains from variable sized packets is difficult because packets with different sizes suffer different delays through a network. Because minProbe does not have control over the application traffic that is used as packet probes, it is important to understand how the accuracy of minProbe changes with different distributions of probe packet sizes. Another consideration is that many estimation algorithms prefer large probe packets to small packets [20, 40].

We evaluate the effect of the length of a probe packet train (i.e. the number of packets in a train) to the accuracy of available bandwidth estimation in Section 4.3.1 and the effect of the distributions of probe packet sizes in Section 4.3.2 and 4.3.3. For these experiments, we always used CBR1 as cross traffic.

	Available Bandwidth [Gbps]							
	Dumb-bell				Parking-lot			
	1.9	3.9	6.9	8.9	1.9	3.9	6.9	8.9
Actual	1.9	3.9	6.9	8.9	1.9	3.9	6.9	8.9
Length	Estimated Available Bandwidth [Gbps]							
5	2.57	5.57	8.54	9.5	1.99	4.41	6.57	8.59
20	2.07	3.96	6.97	8.8	1.80	3.80	6.90	8.30
40	1.9	3.87	6.94	8.68	1.80	3.86	6.70	8.50
60	1.85	3.79	6.79	8.70	1.80	3.80	6.76	8.56
80	1.86	3.79	6.90	8.70	1.80	3.75	6.78	8.44
100	1.83	3.96	6.79	8.55	1.80	3.70	6.56	8.02

Table 5: Estimation with different probe train length.

	Available Bandwidth [Gbps]							
	Dumb-bell				Parking-lot			
	1.9	3.9	6.9	8.9	1.9	3.9	6.9	8.9
Size [B]	Estimated Bandwidth [Gbps]							
64	9.47	9.50	9.50	9.50	9.50	9.50	9.50	9.50
512	2.06	4.51	7.53	8.9	1.85	3.76	6.64	8.09
792	2.07	3.96	6.97	8.8	1.80	3.80	6.90	8.30
1024	1.90	3.97	7.01	8.83	1.80	3.75	6.72	8.54
1518	1.81	3.88	6.91	8.84	1.80	3.81	6.83	8.48

Table 6: Estimation results with different probe packet size.

4.3.1 Impact of Varying Probe Train Length

In order to understand how the number of packets in a probe packet train affects the accuracy of minProbe, we varied the number of packets in each train while using the same parameters as the baseline experiment (Section 4.2). In particular, we used $(N, [0.1 : 0.1 : 9.6]$ Gbps, 10 us, 4 ms) while increasing N from 5 to 100. Table 5 illustrates the estimated available bandwidth when different train lengths were used. The actual available bandwidth is shown in the row marked "Actual" and the estimated available bandwidth is in the rows below "Length" in Table 5. As shown in the table, increasing the number of probe packets per flow yields diminishing returns. A probe train with five packets is not as accurate as the baseline experiment with 20 packets regardless of the actual available bandwidth. However, trains with larger than 20 packets result in similar estimation accuracy. The take-away: Increasing the number of packets in a probe packet train does not necessarily result in more accurate estimation. The minimum number of packets to obtain accurate estimation results was about 20 packets. More packets in a probe train elongate the delay of applications traffic due to buffering, but do not improve estimation accuracy.

What happens when there is not enough packets between a source and destination pair? This highlights the fundamental trade-off between application latency and probing overhead. MinProbe has a timeout mechanism to deal with this corner case. If the oldest intercepted packet has exceeded a pre-defined timeout value, minProbe will generate dummy probe packets to fulfill the need for probe packets and send out the probe train. Since minProbe requires much shorter probe trains compared to existing tools, opportunistically inserting additional dummy packets add minimal overhead.

4.3.2 Impact of Varying Probe Size

Next, we evaluated minProbe with different packet sizes for probes. All the parameters were the same as in the baseline experiment except that we varied the size of packets for probes from 64 bytes to 1518 bytes (the minimum to maximum sized packets allowed by Ethernet). In particular, we used $(20, [0.1 : 0.1 : 9.6]$ Gbps, 10 us, 4 ms) while increasing probe packet sizes from 64 to 1518 bytes. As can be seen from Table 6, larger packet sizes (more than 512 bytes) per-
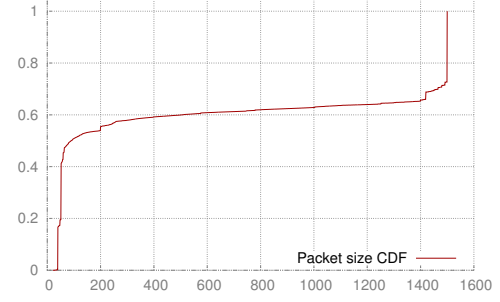

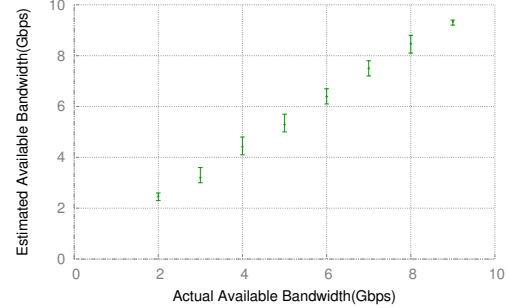Figure 10: The distribution of probe packet sizes from the CAIDA trace.

Figure 11: Estimation with probe packets drawn from the CAIDA trace.

form better than smaller packet sizes in general. Note that we used 792 byte packets in our baseline experiment, which resulted in similar available bandwidth estimate accuracy as 1518 byte probe packets. On the other hand, smaller probe packets, such as 64 byte packets resulted in poor accuracy. This result and observation is consistent with the previous results from literature such as [40]. The take-away is that probe trains with medium to large packet sizes perform better than trains of smaller packet sizes.

4.3.3 Mixed Probe Packet Sizes

In a real network, the distribution of packet sizes is usually mixed with large and small packets. Figure 10 shows the distribution of packet sizes in a recorded Internet trace. We repeat the previous experiment using the baseline setting, except that in this case, we use APP_0 to replay the Internet trace. We let MP_0 modulate the probe train in presence of mixed-sized probe traffic. For each rate $R \in [0.1, 9.6]$, MP_0 ensures that the interpacket gaps between packets of the same flow are uniform. Figure 11 shows the result for CBR1 cross traffic. As can be seen, even though a probe train has mixed packet sizes, the estimation result is still accurate. The reason is that small packets only take a small fraction of total probe train length with respect to large packets. The estimation accuracy is largely determined by the large packets, thus remains accurate.

4.4 Impact of Cross Traffic Characteristics

So far, we have evaluated minProbe under the assumption of constant bit-rate cross traffic. In this section, we no longer make this assumption and instead examine minProbe under bursty cross traffic. In particular, we evaluate minProbe using modeled synthetic bursty traffic (CBR2) and realistic Internet traces.

(a) 1 Gbps
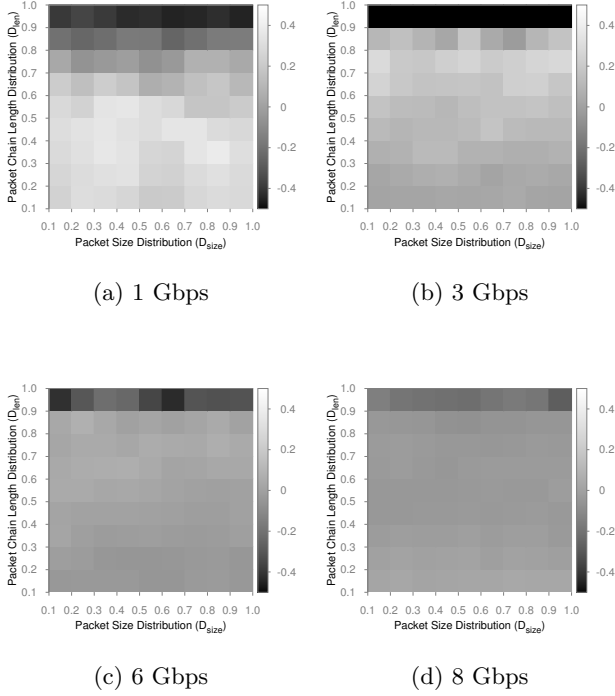
(b) 3 Gbps

(c) 6 Gbps

(d) 8 Gbps

Figure 12: Bandwidth estimation accuracy with different cross traffic burstiness. On y-axis, we turn the knob from no clustering to batching. On x-axis, we turn the knob on cross traffic packet size distribution from uniform distribution to log-normal distribution. We plot the graph for different cross traffic rate: 1Gbps, 3Gbps, 6Gbps and 8Gbps.

4.4.1 Cross Traffic Burstiness

Synthesized Traffic: We first show the results of synthesized bursty cross traffic (CBR2). We generated CBR2 with rate $\in [1, 3, 6, 8]$ Gbps. We set $\mathcal{V}_{size}$ to be a fixed large variance value, e.g. 8×10^4 bytes^2, as specified in [28]. Next, we varied the distribution $\mathcal{D}_{size}$ of packet sizes in CBR2 from 0 to 1 with 0.1 step size. 0 means uniform distribution, 1 means distribution with large variance. Similarly, we varied the distribution $\mathcal{D}_{len}$ of packet chain length in CBR2 from between 0 to 1 with 0.1 step size. Note that even though CBR2 is bursty in terms of the variation of packet distribution, the long term average data rate of CBR2 remains constant.

Figure 12 shows the estimation error (in Gbps) over a range of cross traffic burstiness for four different cross traffic data rates. In each figure, we plot the difference between the actual available bandwidth and the estimated available bandwidth for the cross traffic burstiness identified by the $(\mathcal{D}_{size}, \mathcal{D}_{len})$ parameters. Traffic close to the bottom left corner was more uniformly distributed in both packet sizes and train lengths. Traffic on the top right corner was burstier. Dark gray colors mean under estimation, and light gray colors mean over estimation. As shown in the figure, the estimation error by minProbe is typically within 0.4 Gbps of the true value except when the link utilization is low, or the cross traffic is bursty.

Real Internet Trace: Next, we evaluate minProbe with traces extracted from CAIDA anonymized OC192
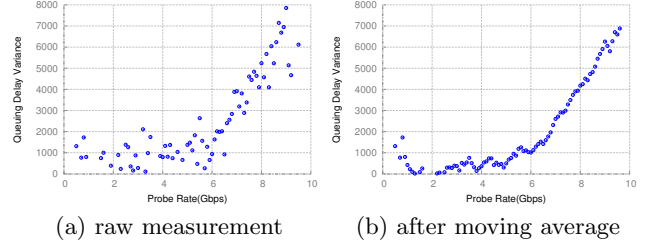

(a) raw measurement

(b) after moving average

Figure 13: Bandwidth estimation of CAIDA trace, the figure on the left is the raw data trace, the figure on the right is the moving average data.

dataset [6], and replayed by SoNIC as a traffic generator. Figure 13a shows an example of the raw data captured by minProbe. We observed that real the traffic traces were burstier than the synthesized traffic in the previous section. To compensate, we used standard exponential moving average (EMA) method to smooth out the data in Figure 13a. For each data points in Figure 13a, the value was replaced by the weighted average of the five data points preceding the current data point. Figure 13b shows the result. Similar to the highly bursty synthesized cross traffic, we achieved a similarly accurate estimation result for the real traffic trace via using the EMA. The estimation error was typically within 0.4Gbps of the true available bandwidth.

In summary, while bursty cross traffic resulted in noisier measurement data than CBR, we were able to compensate for the noise by performing additional statistical processing in the bandwidth estimation. Specifically, we found using the EMA smoothed the measurement data and improved the estimation accuracy. As a result, we observed that cross traffic burstiness had limited impact on minProbe.

4.5 MinProbe In The Wild

In this section, we demonstrate that minProbe works in a wide area Internet network, the National Lambda Rail (NLR). Figure 5 illustrates the experimental network topology. We setup a dedicated route on the NLR with both ends terminating at Cornell University. Node APP_0 generated application traffic, which was modulated by MP_0 using parameter $(N, R, G, D) = (20, [0.1 : 0.1 : 9.6]$ Gbps, 10 us, 4 ms). The traffic was routed through the path shown in Figure 5 across over 2500 miles. Since it was difficult to obtain accurate readings of cross traffic at each hop, we relied on the router port statistics to obtain a 30-second average of cross traffic. We observed that the link between Cleveland and NYC experienced the most cross traffic compared to other links, and was therefore the bottleneck (tight) link of the path. The amount of cross traffic was 1.87 Gbps on average, with a maximum of 3.58 Gbps during the times of our experiments.

Figure 14 shows the result of minProbe in the wild. We highlight two important takeaways: First, the average of our estimation is close to 2 Gbps, which was consistent with the router port statistics collected every 30 seconds. Second, we observed that the readings were very bursty, which means the actual cross traffic on NLR exhibited a good deal of burstiness. In summary, minProbe performed well in the wild, in the wide area. The available bandwidth estimation by minProbe agreed with the link utilization computed from switch port statistical counters: The mean of the minProbe estimation was 1.7Gbps, which was close to the 30-second
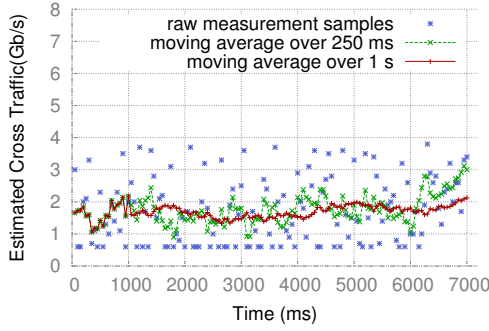
Figure 14: Measurement result in NLR.

average 1.8Gbps computed from switch port statistical counters. Moreover, minProbe estimated available bandwidth at higher sample rate and with finer resolution.

Many cloud datacenters and federated testbeds enforce rate limits on their tenants. For example, the tenants are required to specify the amount of bandwidth to be reserved at the time of provisioning. However, many bandwidth estimation algorithms need to send probe traffic at high data rates to temporarily saturate the bottleneck link. As a result, rate limiting may affect the applicability of the algorithms. We tested the minProbe middlebox inside a federated testbed, ExoGENI, with a virtual network provisioned at 1Gbps on a 10Gbps physical network. We used minProbe to send probe packet trains with different lengths at line rate to find the maximum length of packet train that could be sent before throttled by rate limiters. We found that, in the provisioned 1Gbps virtual network, if the probe train was less than 1200 packets, then there was no observable packet loss. As has been shown in Section 4.3, minProbe only uses probe trains with less than 100 probe packets. As a result, and interestingly, rate limiters do not impact the applicability of minProbe in federate testbed environments.

4.6 Software Router and Other Hardware

Finally, we evaluate whether other middleboxes, such as software routers, can be used to perform high-fidelity network measurements required to accurately estimate available bandwidth without any overhead. In particular, we evaluated two software routers, one based on the Linux kernel network datapath, and another based on the Intel DPDK driver [18]. We configured the software routers to perform L2 forwarding from one port to another. Again, we used the baseline setup, with the exception that software routers were placed between minProbe and the switch. The network path started at the application. After minProbe modulated the application traffic to create packet probe trains, the probe trains were passed through a software router before being sent to a 10 GbE switches.

The experiment was generated from probe packet trains with data rates ranging according to $(N, R, G, D) = (20, [0.5 : 0.5 : 9.5]$ Gbps, 10 us, 4 ms). We show two figures from the this experiment to illustrate the result. First, Figure 15a shows the CDF of the measured instantaneous data rate of probe packet pairs passing through a software router (i.e. we measured the interpacket gap of probe packet pairs after passing through a software router). We configured each software router to forward each packet as soon as it received the packet to minimize any batching. Since we generated an equal number of probe packets (20) for a probe train and
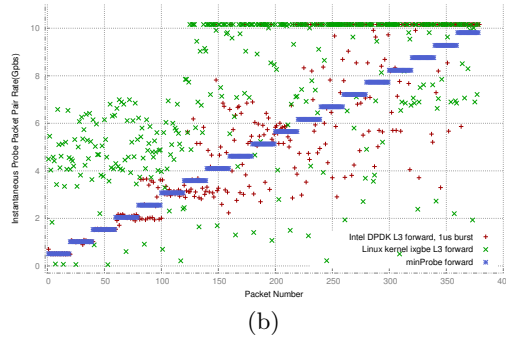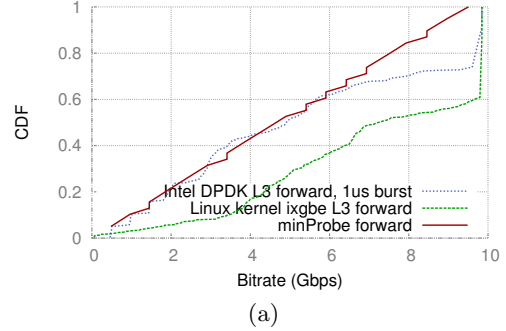

(a)

(b)

Figure 15: Software Routers do not exhibit the same fidelity as minProbe

increased the probe packet train data rate by 0.5 Gbps, the ideal CDF curve should increase along a diagonal frp, 0.5 Gbps to 9.5 Gbps at 0.5 Gbps increments (the red line). However, as seen in the figure, over 25% of the probe packet pairs in the Intel DPDK-based software router were batched with minimum interpacket gap: Batching can be seen via the large increase in the CDF near the highest data rate close to 10 Gbps. Worse, the vanilla kernel datapath (with ixgbe kernel driver) batched over 40% of packets. These results were consistent with the existing research findings that show that network interface cards (NICs) generate bursty traffic at sub-100 microsecond timescale. [25]

Second, Figure 15b highlights the same result but slightly differently. The x-axis is the packet number and the y-axis is the measured instantaneous probe packet pair rate (in Gbps). The figure shows that minProbe was able to modulate interpacket gaps to maintain the required probe data rate (all 20 packets in a probe train exhibited the target data rate), while the software routers were not able to control the probe rate at all. To summarize, due to batching, software routers are not suitable for performing the required high-fidelity available bandwidth estimation on high-speed networks.

Next, we investigated the question if prior work such as MGRP [37] could perform on high-speed networks? To answer this, we setup MGRP to perform the same baseline estimation experiment in Figure 8. Unfortunately, the result was consistent with our findings above and in Figures 15a and 15b. In particular, we found that MGRP could not report valid results when it was used in high-speed networks (10Gbps Ethernet). The accuracy of MGRP was limited by its capability to precisely timestamp the received probe packets and its ability to control the probe packet gaps. Both of these capabilities were performed at kernel level in MGRP and were prone to operating system level noise. The accu-
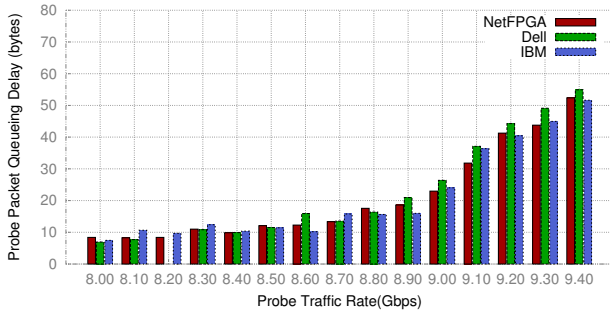
Figure 16: Estimating Available Bandwidth on different switches

racy of MGRP was better than Pathload [20], it eliminated the overhead of extra probing traffic, but the fundamental accuracy was still constrained by the measurement platform.

Finally, we studied the sensitivity of bandwidth estimation with respect to network hardware. In particular, we experimented with three different 10 GbE switches: IBM G8264T, Dell S4810, and NetFPGA-10G reference switch design [31]. We used the baseline setup for all experiments and configured all three switches to perform L2 forwarding. Figure 16 illustrates an example of captured queuing delay after each hardware. As can be seen from the figure, the three switches can be used nearly interchangeably since there was no significant difference in queuing delay. As a result, we have found that the underlying hardware itself may not contribute to the available bandwidth estimation. Instead, as earlier results in the paper indicate, the fidelity of the available bandwidth estimation depend more on the ability to control generated interpacket gaps and measure received interpacket gaps.

5. DISCUSSION

In this section, we discuss the issues regarding the deployment of minProbe, the applications of available bandwidth estimation, and whether minProbe can be generalized to measure bandwidth in 1GbE and 40GbE.

5.1 Deployment

Middleboxes are widely deployed in datacenter networks to perform a wide spectrum of advanced network processing functions ranging from security (firewalls, intrusion detection), traffic shaping (rate limiters, load balancers), to improving application performance (accelerators, proxies, caches), to name a few. Similarly, minProbe deployment scenarios include middleboxes with enhanced measurement capabilities potentially located in the same rack as other servers, or even integrated into each server directly, possibly using hypervisor-based network virtualization, provided that there exists proper support for accessing the physical layer of the network in software. In the future, we will explore the possibility of deploying minProbe as a platform for providing high-fidelity network measurement as a service (NMaaS).

5.2 Virtualization and Availability Bandwidth Estimation

Because of virtualization, datacenter tenants no longer have direct access to the underlying physical network. The

extra layer of indirection makes it hard to optimize application performance. MinProbe could potentially bridge the gap. It can measure the underlying network and provide performance metrics to the virtualized applications to optimize tasks such as VM placement and route selection.

5.3 Generalization to 1GbE and 40GbE

At the time of writing, minProbe operated only in 10 GbE networks. However, the high-fidelity capability of minProbe can be extended to support 1GbE and 40GbE networks as well. The architecture of the PHY for 40GbE networks is very similar to the PHY in a 10GbE network. As a result, as future work, we intend to extend minProbe to support 40GbE. Support for 40GbE networks will require parallelizing the processing the PHY layer functionality using modern multi-core architecture. Moreover, as future work, we intend to extend minProbe to support 1GbE networks. The PHY for 1GbE networks are less complicated than 10GbE PHY, which makes it possible to port minProbe to 1GbE. For example, the encoding and decoding schemes at physical coding layer in 1GbE is simpler than the 10GbE physical coding layer.

5.4 GENI

MinProbe is available on ExoGENI [10]. Users can provision compute nodes that has SoNIC cards installed and use it as a minProbe to run network measurement experiments. Currently, at the time of writing, minProbe was enabled at two ExoGENI sites: RENCI (Renaissance Computing Institute) and University of California, Davis. We are in the process of expanding to more sites in the near future.

6. RELATED WORK

Prior work in MAD [43], MGRP [37] and Periscope [15] provide a thin measurement layer (via userspace daemon and kernel module) for network measurement in a shared environment. These works complement minProbe. MinProbe is applicable in a shared environment. We also advance the conversation of available bandwidth estimation to 10Gbps, unlike most of the prior work, which were only demonstrated to operate in 1Gbps or less.

We use an algorithm similar to Pathload [20] and Pathchirp [40] to estimate available bandwidth. There are many related works on both theoretical and practical aspect of available bandwidth estimation [7, 20, 23, 29, 30, 32, 38, 40, 42, 44]. Our work contributes more on the practice of available bandwidth estimation in high speed network (10Gbps). We found that existing probing parameterizations such as probe trains are sound and still applicable in high-speed networks when supported by the appropriate instrumentation. Furthermore, [21, 48] mentioned that burstiness of the cross traffic can negatively affect the accuracy of estimation. While we found that bursty traffic introduces noise into the measurement data, the noise can be filtered out using simple statistical processing, such as the moving average.

Middleboxes are popular building blocks for current network architecture [41]. MinProbe, when operating as a middlebox, is similar to software routers in a sense that minProbe consists of a data forwarding path and programmable flow table. Unlike software routers, which typically focus on high throughput, minProbe has the capability to precisely control the distance between packets; this capability is absent in most existing software routers. From the system de-

sign perspective, ICIM [34] has proposed a similar inline network measurement mechanism as our middlebox approach. However, ICIM has only simulated their proposal, while we implemented a prototype and performed experiment in real network. Others have investigated the effect of interrupt coalescence [39] and memory I/O subsystem [24], but they are orthogonal to our efforts. MinProbe, albeit a software tool, avoids the noise of OS and network stack completely by operating at the physical layer of the network stack.

Another area of related work is precise traffic pacing and precise packet timestamping. They are useful system building blocks for designing a high-fidelity network measurement platform. Traditionally, traffic pacing [8] is used to smooth out the burstiness of the traffic to improve system performance. In minProbe, we use traffic pacing in the opposite way to generate micro-burst of traffic to serve as probe packets. Precise timestamping has been used widely in passive network monitoring. Typically, this is achieved by dedicated hardware platform, such as Endace Data Acquisition and Generation (DAG) card [1]. With minProbe, we achieve the same nanosecond timestamping precision, and we are able to use the precise timestamp for active network measurement, which the traditional hardware platform are incapable of.

7. CONCLUSION

Available bandwidth estimation as a research topic has been studied extensively, but there still lacks an accurate and low cost solution in high-speed networks. We present minProbe, which is a high-fidelity, minimal-cost and userspace accessible network measurement approach that is able to accurately measure available bandwidth in 10 gigabit-persecond (Gbps) networks. We provided a systematic study of minProbe's performance with respect to various cross traffic and probe traffic conditions and patterns. We found that minProbe performs well even under bursty traffic, and the estimation is typically within 0.4 Gbps of the true value in a 10 Gbps network.

8. AVAILABILITY

The *minProbe* and SoNIC source code is published under a BSD license and is freely available for download at `http://sonic.cs.cornell.edu`. SoNIC nodes are available for experimentation as bare-metal nodes at the following ExoGENI sites: RENCI and UCDavis.

9. ACKNOWLEDGMENTS

10. REFERENCES

[1] Endace DAG Network Cards. `http://www.endace.com/endace-dag-high-speed-packet-capture-cards.html`.

[2] High Frequency sFlow v5 Counter Sampling. `ftp://ftp.netperf.org/papers/high_freq_sflow/hf_sflow_counters.pdf`.

[3] IEEE Standard 802.3-2008. `http://standards.ieee.org/about/get/802/802.3.html`.

[4] Linux programmer's manual. `http://man7.org/linux/man-pages/man7/netlink.7.html`.

[5] sflow, version 5. `http://www.sflow.org/sflow_version_5.txt`.

[6] The CAIDA UCSD Anonymized Internet Traces. `http://www.caida.org/datasets/`.

[7] Ahmed Ait Ali, Fabien Michaut, and Francis Lepage. End-to-End Available Bandwidth Measurement Tools : A Comparative Evaluation of Performances. *arXiv.org*, June 2007.

[8] Mohammad Alizadeh, Abdul Kabbani, Tom Edsall, Balaji Prabhakar, Amin Vahdat, and Masato Yasuda. Less is more: Trading a little bandwidth for ultra-low latency in the data center. In *Procs. NSDI*, 2012.

[9] Bilal Anwer, Theophilus Benson, Nick Feamster, Dave Levin, and Jennifer Rexford. A slick control plane for network middleboxes. In *HotSDN*, 2013.

[10] Mark Berman, Jeffrey S. Chase, Lawrence Landweber, Akihiro Nakao, Max Ott, Dipankar Raychaudhuri, Robert Ricci, and Ivan Seskar. Geni: A federated testbed for innovative network experiments. *Comput. Netw.*, 61:5–23, March 2014.

[11] Mihai Dobrescu, Norbert Egi, Katerina Argyraki, Byung-Gon Chun, Kevin Fall, Gianluca Iannaccone, Allan Knies, Maziar Manesh, and Sylvia Ratnasamy. Routebricks: exploiting parallelism to scale software routers. In *Proc. SOSP*, 2009.

[12] Daniel A. Freedman, Tudor Marian, Jennifer H. Lee, Ken Birman, Hakim Weatherspoon, and Chris Xu. Exact temporal characterization of 10 gbps optical wide-area network. In *Proc. IMC*, 2010.

[13] Cesar D. Guerrero and Miguel A. Labrador. On the applicability of available bandwidth estimation techniques and tools. *Comput. Commun.*, 33(1):11–22, January 2010.

[14] Sangjin Han, Keon Jang, KyongSoo Park, and Sue Moon. Packetshader, a gpu-accelerated software router. In *Proc. SIGCOMM*, 2010.

[15] Khaled Harfoush, Azer Bestavros, and John Byers. Periscope: An active internet probing and measurement api. Technical report, Boston University Computer Science Department, 2002.

[16] Ningning Hu, Li Erran Li, Zhuoqing Morley Mao, Peter Steenkiste, and Jia Wang. Locating internet bottlenecks: algorithms, measurements, and implications. In *Proc. SIGCOMM, 2004*, 2004.

[17] Péter Hága, Attila Pásztor, Darryl Veitch, and István Csabai. Pathsensor: Towards efficient available

bandwidth measurement. In *Proc. IPS-MoMe 2005*, 2005.

[18] Intel DPDK. `http://www.dpdk.com`.

[19] Intel Westmere. `http://ark.intel.com/products/codename/33174/Westmere-EP`.

[20] M Jain and C Dovrolis. Pathload: A Measurement Tool for End-to-End Available Bandwidth. 2002.

[21] Manish Jain and Constantinos Dovrolis. Ten fallacies and pitfalls on end-to-end available bandwidth estimation. In *Proc. IMC*, 2004.

[22] Hao Jiang and Constantinos Dovrolis. Why is the internet traffic bursty in short time scales? In *Proc. SIGMETRICS*, 2005.

[23] Guojun Jin and Brian L. Tierney. System capability effects on algorithms for network bandwidth measurement. Proc. IMC, 2003, New York, NY, USA, 2003. ACM.

[24] Guojun Jin and Brian L. Tierney. System capability effects on algorithms for network bandwidth measurement. In *Proc. IMC*, 2003.

[25] Rishi Kapoor, Alex C. Snoeren, Geoffrey M. Voelker, and George Porter. Bullet trains: A study of nic burst behavior at microsecond timescales. In *Proc. CoNEXT*, 2013.

[26] Ki Suh Lee, Han Wang, and Hakim Weatherspoon. Sonic: Precise realtime software access and control of wired networks. In *Proc. NSDI*, 2013.

[27] Ki Suh Lee, Han Wang, and Hakim Weatherspoon. Phy covert channels: Can you see the idles? In *Proc. NSDI*, 2014.

[28] ChiunLin Lim, KiSuh Lee, Han Wang, Hakim Weatherspoon, and Ao Tang. Packet clustering introduced by routers: modelling, analysis and experiments. In *Proc. CISS*, 2014.

[29] Xiliang Liu, Kaliappa Ravindran, Benyuan Liu, and Dmitri Loguinov. Single-hop probing asymptotics in available bandwidth estimation: sample-path analysis. In *Proc. IMC*, 2004.

[30] Xiliang Liu, Kaliappa Ravindran, and Dmitri Loguinov. Multi-hop probing asymptotics in available bandwidth estimation: stochastic analysis. In *Proc. IMC*, October 2005.

[31] John W. Lockwood, Nick McKeown, Greg Watson, Glen Gibb, Paul Hartke, Jad Naous, Ramanan Raghuraman, and Jianying Luo. NetFPGA–An Open Platform for Gigabit-Rate Network Switching and Routing. In *Proceedings of Microelectronics Systems Education*, 2007.

[32] Sridhar Machiraju. *Theory and Practice of Non-Intrusive Active Network Measurements*. PhD thesis, EECS Department, University of California, Berkeley, May 2006.

[33] Sridhar Machiraju and Darryl Veitch. A measurement-friendly network (mfn) architecture. In *Proc. SIGCOMM INM*, Pisa, Italy, 2006.

[34] Cao Le Thanh Man, G. Hasegawa, and M. Murata. Icim: An inline network measurement mechanism for highspeed networks. In *Proceedings of the 4th IEEE/IFIP Workshop on End-to-End Monitoring Techniques and Services*, April 2006.

[35] Tudor Marian, Ki Suh Lee, and Hakim Weatherspoon. Netslices: scalable multi-core packet processing in user-space. In *Proc. ANCS*, 2012.

[36] B. Melander, M. Bjorkman, and P. Gunningberg. A new end-to-end probing and analysis method for estimating bandwidth bottlenecks. In *IEEE Global Telecommunications Conference*, 2000.

[37] Pavlos Papageorge, Justin McCann, and Michael Hicks. Passive aggressive measurement with mgrp. *SIGCOMM Comput. Commun. Rev.*, 39(4):279–290, August 2009.

[38] R Prasad, C Dovrolis, M Murray, and K Claffy. Bandwidth estimation: metrics, measurement techniques, and tools. *Network*, 2003.

[39] Ravi Prasad, Manish Jain, and Constantinos Dovrolis. Effects of interrupt coalescence on network measurements. In *Proceedings of Passive and Active Measurements Workshop*, 2004.

[40] V Ribeiro, R Riedi, R Baraniuk, and J Navratil. pathchirp: Efficient available bandwidth estimation for network paths. In *Proc. PAM*, 2003.

[41] Vyas Sekar, Sylvia Ratnasamy, Michael K. Reiter, Norbert Egi, and Guangyu Shi. The middlebox manifesto: Enabling innovation in middlebox deployment. In *Proc. HotNet*, 2011.

[42] J Sommers, P Barford, and W Willinger. Laboratory-based calibration of available bandwidth estimation tools. *Microprocessors and Microsystems*, 31(4):222–235, 2007.

[43] Joel Sommers and Paul Barford. An active measurement system for shared environments. In *IMC*, 2007.

[44] Joel Sommers and Paul Barford. An active measurement system for shared environments. In *Proc. IMC, 2007*, October 2007.

[45] Joel Sommers, Paul Barford, and Mark Crovella. Router primitives for programmable active measurement. In *In Proc. PRESTO*, 2009.

[46] Jacob Strauss, Dina Katabi, and Frans Kaashoek. A Measurement Study of Available Bandwidth Estimation Tools. In *Proc. SIGCOMM*, 2003.

[47] Kashi Venkatesh Vishwanath and Amin Vahdat. Realistic and responsive network traffic generation. In *Proc. SIGCOMM*, 2006.

[48] Kashi Venkatesh Vishwanath and Amin Vahdat. Evaluating distributed systems: Does background traffic matter? In *Proc. USENIX ATC*, 2008.

[49] Yong Xia, Lakshminarayanan Subramanian, Ion Stoica, and Shivkumar Kalyanaraman. One more bit is enough. *SIGCOMM Comput. Commun. Rev.*, 35(4):37–48, August 2005.

[50] Curtis Yu, Cristian Lumezanu, Yueping Zhang, Vishal Singh, Guofei Jiang, and Harsha V. Madhyastha. Flowsense: Monitoring network utilization with zero measurement cost. In *In Proc. PAM*, 2013.